

# COMMISSIONING OF ATLAS AND EARLY MEASUREMENTS WITH LEPTONS IN ATLAS AND CMS

M. PLAMONDON

*LAL, Univ Paris-Sud, IN2P3/CNRS, Orsay, France  
on behalf of ATLAS and CMS collaborations*

With only a few months until the LHC start-up, the commissioning of ATLAS is in its final stage as the last components of the detector are installed. The understanding of the detector response acquired during the preparation phase is presented as well as the expected performance at start-up. The strategies of both ATLAS and CMS regarding the use of early data involving leptons is then described. Assuming an integrated luminosity of  $100 \text{ pb}^{-1}$  in 2008, examples of calibration procedures and early measurements are given.

## 1 Commissioning of ATLAS

At the time of this paper, everything except the endwall muon chambers has been installed. In this section we summarize the acquired understanding of the detector performance before start-up.

### 1.1 Detector status at start-up

The endwall muon chambers are the last components to be installed in the cavern (June 2008). With the full magnet tests performed soon afterwards in order to check the endcap toroids at their nominal field, the entirety of the ATLAS detector will have been assembled ready for the first collisions. Data taking has already been tested with cosmic rays throughout the two preceeding years of commissioning as the different detectors have been installed. The complete acquisition and processing chain has been successfully exercised from the primary site at CERN and throughout worldwide distributed sites.

### 1.2 Inner detectors

The commissioning of the Inner Detector was initiated on the surface where cabling checks and debugging were performed. Once in the cavern, the noise levels were the same as those measured on the surface. The global alignment between the silicon strip (SCT) and transition radiation (TRT) trackers was measured with reconstructed cosmic ray tracks (as shown in Fig.1), where the results were consistent with precision survey measurements. Little time was available for cabling cross-checks of the innermost layer of pixels which was cabled just before ATLAS was closed. The number of non-working channels was measured to be small (0.3%).

### 1.3 Calorimeters

The calorimeters went down into the cavern beginning in 2006 and have been operating under stable conditions for a long period of time. For example, the liquid argon calorimeter was cold (88K) with a measured temperature variation of 10 mK for over a year. The degree of understanding of the detector response is well illustrated by cosmic rays. Large signals as in Fig.1 are frequently observed, interpreted as muons emitting a bremsstrahlung photon in the calorimeters. These events have allowed timing studies (channel intercalibration at the level of 2 ns) as well as improving the description of the pulse shape. In general, muons are minimum ionising particles and deposit energy according to a Landau distribution. By analyzing these distributions, the uniformity of response across EM readout channels could be cross-checked to the 2% level<sup>1</sup>. Taking advantage of the several months of commissioning running, many problems were identified and corrected, leaving only a small fraction of defective channels ( $\sim 0.1\%$  in the case of the LAr calorimeter).

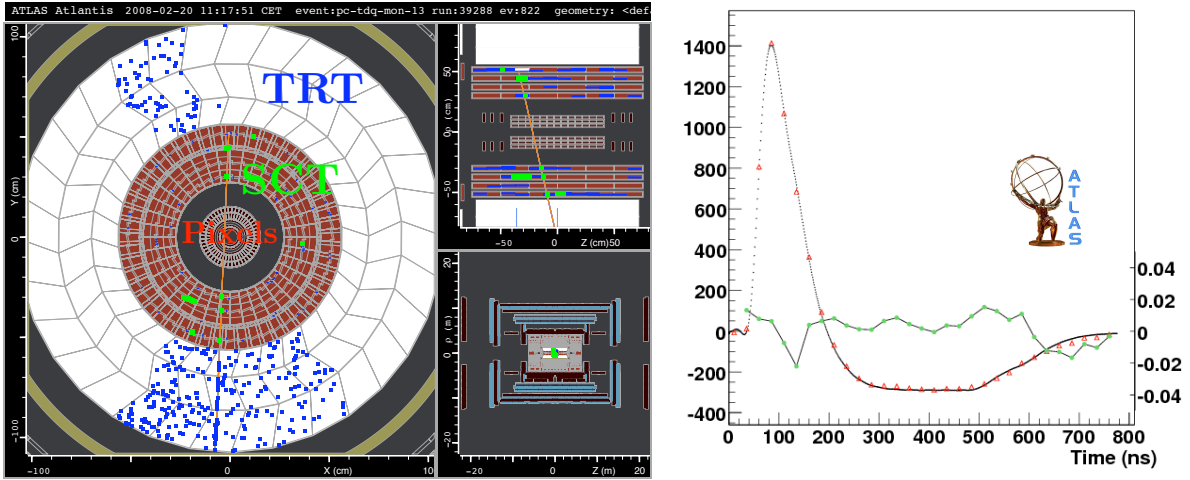


Figure 1: On the left is shown the trajectory of a cosmic muon reconstructed in the inner detectors. No zero suppression being performed, this display reveals that only a fraction of the TRT was recording data. The right plot shows a large amplitude signal ( $\sim 13$  GeV) in the LAr calorimeter which was also recorded during the commissioning. Compared to the predicted pulse, the residual in green is showing good agreement at the percent level.

### 1.4 Muon spectrometer

The commissioning of the muon spectrometer was aimed at testing its complex alignment system using optical sensors. The alignment is of crucial importance as a 1 TeV muon is bent only by  $500 \mu\text{m}$  under the magnetic field produced by the toroids. In order to reach 10% accuracy on the momentum measurement, the chambers must be aligned with a precision of  $50 \mu\text{m}$ . After a calibration of the system by moving and rotating modules, the reconstructed cosmic tracks have shown that the misalignments can be well monitored.

## 2 Early physics with leptons

With the first collisions, the main goal will be to calibrate the detectors *in situ* using well-known physics samples. Table 1 summarizes the expected performances at start-up and those expected to be ultimately reached. The rediscovery of standard model at  $\sqrt{s} = 10$  TeV will be followed by an effort to validate and tune the MC generators. Leptons will play a crucial

role in paving the way to new physics, taking half the trigger rate of the foreseen menu at  $\mathcal{L} = 10^{31} \text{ cm}^{-2} \text{ s}^{-1}$ . Assuming 3 months of operation in 2008 and an integrated luminosity around  $100 \text{ pb}^{-1}$ , calibration procedures and possible early measurements are described in the following.

		Performance		Physics goals	Physics signals tools
		@ start-up	nominal		
EM energy uniformity	ATLAS	$\lesssim 1\text{-}2\%$	0.7%	$H \rightarrow \gamma\gamma$	isolated $e$ , $Z \rightarrow ee$ $\phi$ -symmetry
	CMS	$\lesssim 2\text{-}4\%$	0.5%		
EM energy scale		$\sim 2\%$	0.02%	$W$ mass	$Z \rightarrow ee$
Inner detector alignment		$50\text{-}100 \mu\text{m}$	$<10 \mu\text{m}$	$b$ -tagging	isolated $\mu$ , $Z \rightarrow \mu\mu$
Muon system alignment		$<200 \mu\text{m}$	$30 \mu\text{m}$	$Z' \rightarrow \mu\mu$	$Z \rightarrow \mu\mu$
Muon momentum scale		$\sim 1\%$	0.02%	$W$ mass	$Z \rightarrow \mu\mu$

Table 1: This table summarizes the detector performance concerning leptons which are expected at start-up. The values, mostly given for the ATLAS case, are compared to those ultimately reached using the physics tools mentioned in the last column.

## 2.1 First peaks: $(J/\psi, \Upsilon, Z) \rightarrow \mu\mu$

Assuming a 30% overall detector and machine efficiency at  $10^{31} \text{ cm}^{-2} \text{ s}^{-1}$ , around 16000  $J/\psi$  and 3000  $\Upsilon$  in dimuons are accumulated per  $\text{pb}^{-1}$ , useful to perform checks, tracker alignment and momentum scale determination. After all cuts,  $\sim 600 Z \rightarrow \mu\mu$  events are also recorded. As shown in figure 2, the measured  $Z$  boson mass is sensitive to misalignments of the tracker or the muon system as well as uncertainties on the magnetic field (distorted B field): a misaligned tracker would affect noticeably the shape of the  $Z$  peak.

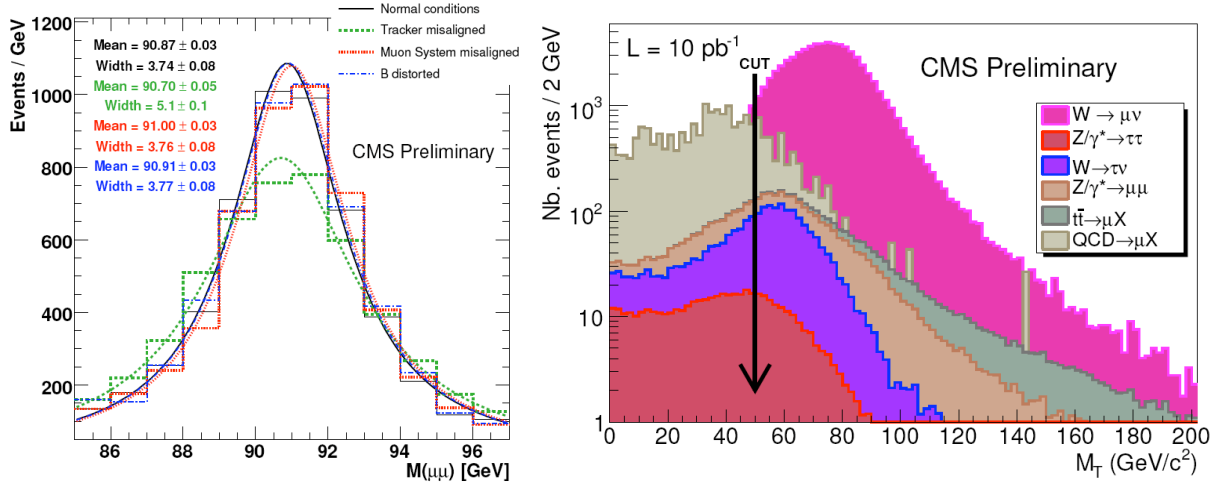


Figure 2: A peak of  $\sim 6000 Z$  obtained with  $10 \text{ pb}^{-1}$  is the starting point of many studies of the muon system as shown on the left in the case of CMS (the same effects exist in ATLAS). A clear  $W$  peak is obtained as well (right). A cut at 50 GeV on the transverse mass ( $M_T$ ) gives a clean  $W$  sample that can be used for  $\cancel{E}_T$  studies.

## 2.2 $Z \rightarrow ee$ calibration and energy scale

Simple analysis cuts are used to obtain the first  $Z$  and  $W$  samples with low background levels as in figure 2 (right). For example, they can be done without the tracker or restricted to the barrel region if required. The  $Z$ -mass constraint is a key tool for the commissioning of electron

reconstruction and will also be used to correct residual long-range non-uniformities. From the design of ATLAS LAr calorimeter, relatively large regions ( $0.2 \times 0.4$  in  $\eta \times \phi$ ) are expected to be locally uniform and this was demonstrated from testbeam data<sup>2</sup>. In order to intercalibrate them,  $\sim 30000$   $Z \rightarrow ee$  events will be sufficient to achieve the desired response uniformity of  $\sim 0.7\%$  (see Fig.3). The situation in CMS<sup>3</sup> is different due to the crystal-to-crystal response which varies by  $\gtrsim 2\%$ . Higher statistics ( $\sim 10 \text{ fb}^{-1}$ ) are required to perform a similar intercalibration.

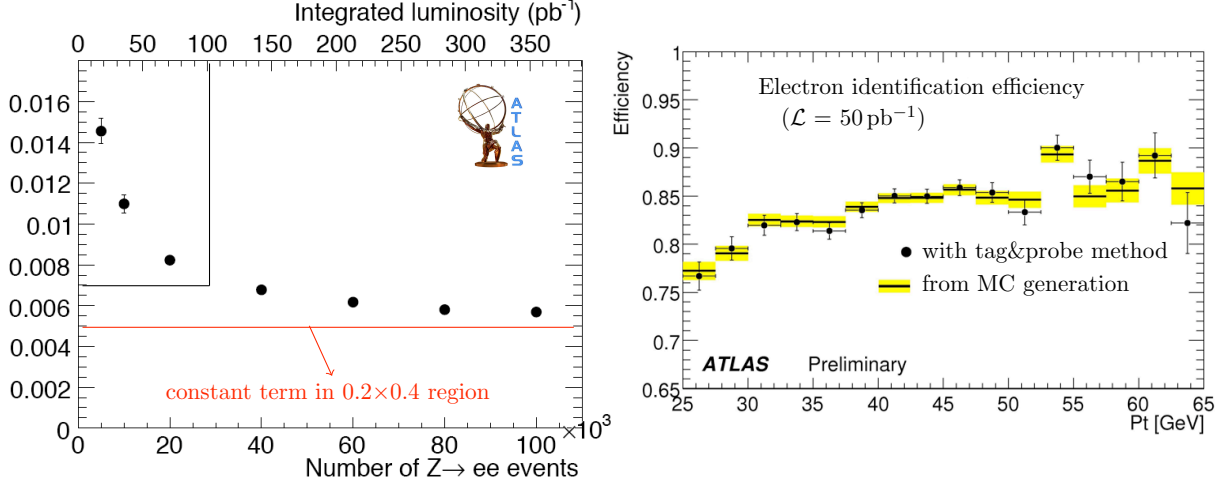


Figure 3: The ATLAS EM intercalibration as a function of the integrated luminosity (left) reaches 0.7% at about  $100 \text{ pb}^{-1}$ . In the right plot, the efficiency of selecting electrons in ATLAS is accurately evaluated using the tag&probe method described in the text (1% agreement w.r.t. MC generation).

### 2.3 $Z$ and $W$ cross-sections

The expected precision for ATLAS and CMS in the measurements of the  $Z$  and  $W$  cross-sections (table 2) are limited by statistical uncertainties. Theoretical uncertainties remain at 2%, mainly due to acceptance determination and PDFs. The luminosity uncertainty of 10% will dominate until the dedicated detectors<sup>4,5</sup> refine these measurements in 2009. Systematics are kept to the 1% level with efficiency precisely determined using data-driven methods (tag&probe) as illustrated in Fig.3 in the case of electron identification. In simulated  $Z$  events, an electron candidate is tagged by fulfilling stringent isolation and reconstruction requirements. A simple object is then looked for on the opposite side, either a track or an EM cluster. If the invariant mass of the pair falls in the mass window of the  $Z$  ( $M_{ee} = M_Z \pm 20 \text{ GeV}$ ), the latter is known to be an electron and the efficiency can be computed in this way.

process		$\frac{\Delta\sigma}{\sigma}$
$Z/\gamma^* + X \rightarrow \mu\mu$	ATLAS	$0.004(\text{stat}) \pm 0.008(\text{sys}) \pm 0.02(\text{th}) \pm 0.1(\text{lumi})$
	CMS	
$W \rightarrow e\nu$	ATLAS	$0.002(\text{stat}) \pm 0.050(\text{sys})$ //

Table 2: The various contributions to the uncertainty of cross-section measurements are given for  $50 \text{ pb}^{-1}$  of integrated luminosity. Higher systematic uncertainties are expected in the case of  $\sigma_W$ , especially from the  $\cancel{E}_T$  measurement.

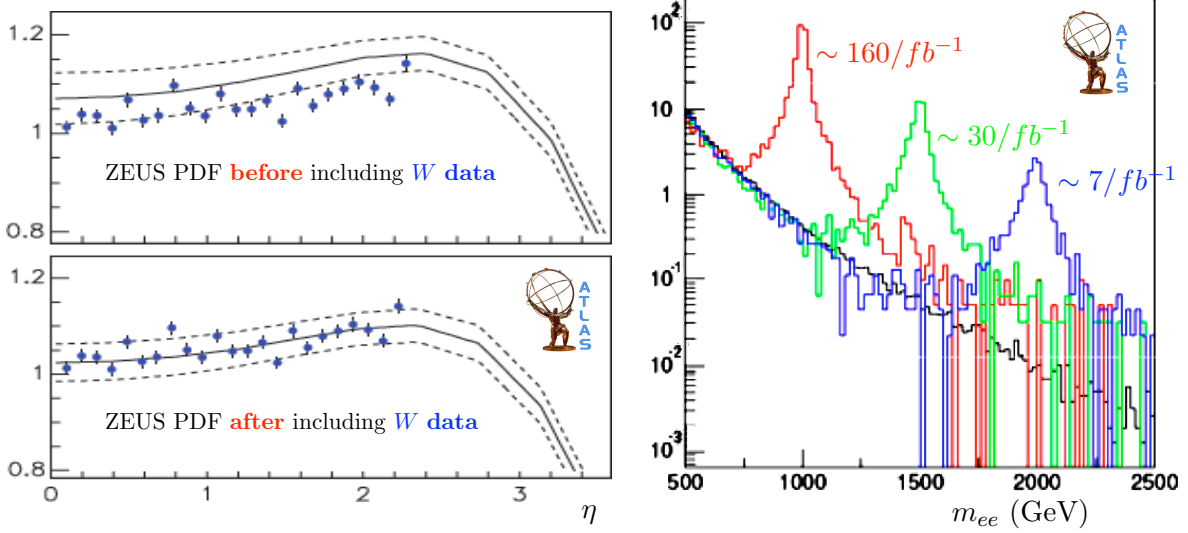


Figure 4: The electron rapidity distributions in  $W$  decays can be used to constrain PDF distributions (left). Dielectron resonances at the TeV scale could be seen with a fraction of the statistics shown here for  $1 \text{ fb}^{-1}$  (right).

#### 2.4 Constrain PDFs with $W \rightarrow \ell\nu$

A region of the  $x - Q^2$  plane becomes accessible at the LHC with a higher centre-of-mass energy ( $x_{1,2} = \frac{M}{\sqrt{s}}e^{\pm y}$ ). For instance, the  $W$  production would involve  $10^{-4} < x_{1,2} < 0.1$ , a region dominated by sea-sea parton interactions. At these low  $x$  values, the current PDF uncertainties remain large (4-8%<sup>6</sup>). By adding LHC data into global fits, it would be possible to constrain further the PDFs. With a 5% experimental precision,  $e^{\pm}$  angular distributions could be used to discriminate between different PDF parametrizations. The principle is demonstrated by generating  $10^6 W \rightarrow e\nu$ , equivalent to  $150 \text{ pb}^{-1}$  of data. These simulated events are generated with the CTEQ6.1 PDF and full detector simulation. Statistical uncertainty being negligible, only a 4% systematic error is introduced by hand, a level already attained with the  $Z \rightarrow ee$  sample. These pseudo-data are included in the global ZEUS PDF fit in order to assess their impact. The uncertainty on the low- $x$  gluon shape parameter  $\lambda$  [ $xg(x) \sim x^{-\lambda}$ ] is reduced by 40%.

#### 2.5 Leptons for early top

The easiest channel to consider at the beginning is one lepton plus jets ( $t\bar{t} \rightarrow b\ell\nu bj\bar{j}$ ) with  $t\bar{t}$  combinatorics,  $W$ +jets and QCD as main backgrounds. The b-tagging will not be available at start-up and  $\cancel{E}_T$  might be problematic as well. For these reasons, early top analyses are *lepton-triggered*. Nevertheless, a signal can be quickly seen with only  $\sim 10 \text{ pb}^{-1}$ , even with limited detector performance and a simple analysis. With  $100 \text{ pb}^{-1}$ , these early measurements of  $\delta\sigma_{t\bar{t}}$  will reach  $\sim 20\%$  and  $\delta m_{top}$  at  $< 10 \text{ GeV}$ . It will be an excellent sample for light jet calibration and b-jet efficiency determination.

#### 2.6 Early discoveries with leptons?

The discovery of a narrow resonance decaying to  $e^+e^-$  (Fig.4) is accessible with as few as  $70 \text{ pb}^{-1}$  if  $M \simeq 1 \text{ TeV}$ . At these energies, ultimate calorimeter performance is not needed. Early searches in the case of dimuons decays would be less straightforward since the resolution worsens as  $p_T$  increases. However, the generally lower instrumental background may make dimuons a discovery channel along with dielectrons.

### 3 Conclusions

ATLAS has been commissioning its detector with cosmic rays and is eagerly awaiting the first LHC collisions in 2008. The clean signatures involving leptons will have a major impact in the initial understanding of the detectors. Summarized in figure 5, the early physics program involves several activities with possible surprises along the way.

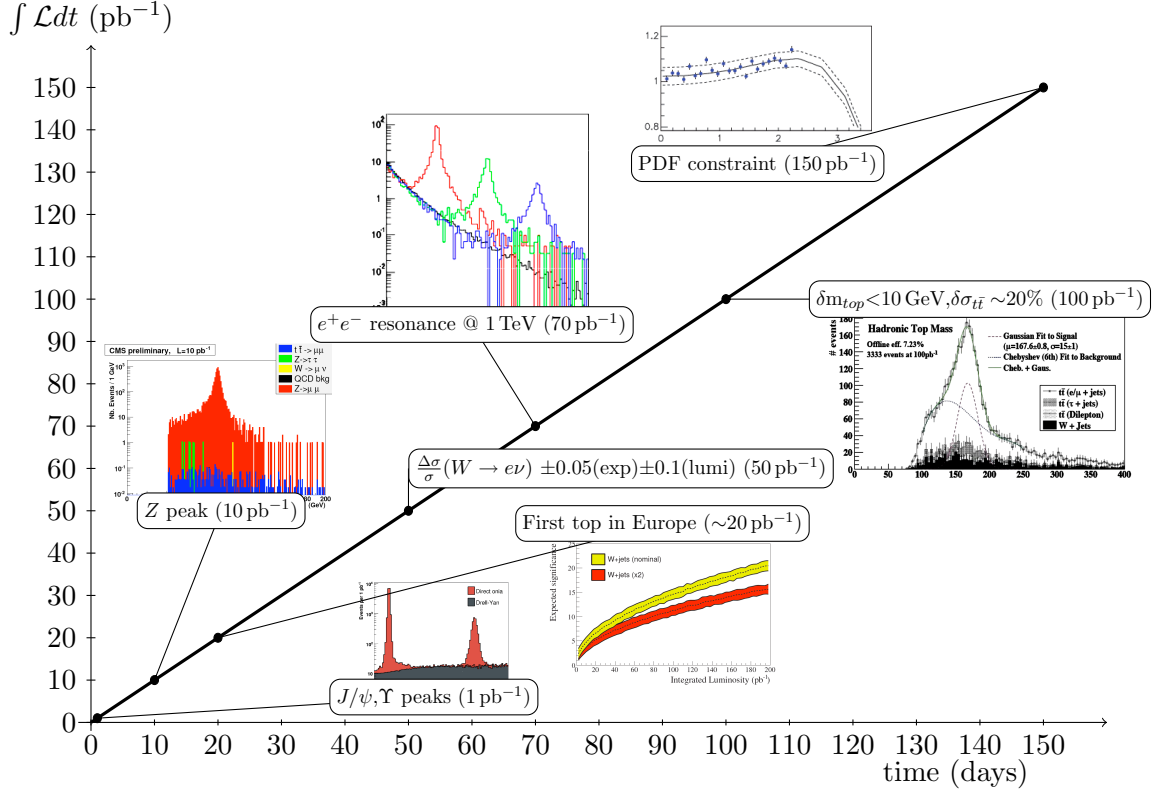


Figure 5: Summary of the physics program with the first year of LHC data taking.

### References

1. M. Cooke et al. In situ commissioning of the atlas electromagnetic calorimeter with cosmic muons. Technical Report ATL-LARG-PUB-2007-013. ATL-COM-LARG-2007-012, CERN, Geneva, Nov 2007.
2. J. Colas et al. Response Uniformity of the ATLAS Liquid Argon Electromagnetic Calorimeter. *Nucl. Instrum. Meth.*, A582:429–455, 2007.
3. G. L. Bayatian et al. CMS physics: Technical design report. CERN-LHCC-2006-001.
4. V. Berardi et al. TOTEM: Technical design report - Addendum. Total cross section, elastic scattering and diffraction dissociation at the Large Hadron Collider at CERN. CERN-LHCC-2004-020.
5. Peter Jenni, Markus Nordberg, Marzio Nessi, Kerstin Jon-And, , and and. Atlas forward detectors for measurement of elastic scattering and luminosity. 2008. CERN-LHCC-2008-004.
6. Amanda Cooper-Sarkar and Claire Gwenlan. Comparison and combination of ZEUS and H1 PDF analyses. 2005. hep-ph/0508304.